IEICE TRANS. COMMUN., VOL.E94–B, NO.9 SEPTEMBER 2011

LETTER *Special Section on Information Communication Technology for Highly Reliable Human Health Care Services*

On-Body Area UWB Channel Modeling Including Reflection from Surroundings

Ippei KIMURA[†], *Nonmember and* **Jianqing WANG**[†a)], *Member*

SUMMARY This study aims how to contain the environment reflection in a dynamic on-body ultra wideband (UWB) channel model. Based on a measurement approach, it is demonstrated that a complete body area channel model can be regarded as a combination of the on-body propagation characteristic and additional components from the environment. Based on such a channel model, the effect of environment reflection on the average bit error rate performance was investigated for a typical impulse radio UWB system.

key words: *wireless body area network, ultra wideband, channel model, environment reflection*

1. Introduction

Along with a wide-scale demand for more advanced healthcare and medical treatment, there is a new possibility of high-quality service from hospitals by linking variousredbiotical sensors to establish a body area network of personal health information. For such a body area network, the ultra wideband (UWB) technology is attracting much attention because its feature agrees with the requirement for low power, high speed and short range body area communications.

When designing a body area network system, a statistical on-body channel model is essential [2]–[4]. Especially, a dynamic channel model with various body posture effects [5] is indispensable in a practical healthcare or medical treatment scenario. However, most of the present channel models are limited either only the human body or only the environment reflection. For the latter, Molisch et al. have made a comprehensive review for indoor UWB channel models in which the reflection from surroundings should be a dominant factor of multipaths [6], [7]. However, it is unclear to how to combine the on-body propagation and the environment reflection into a complete channel model. In this study, based on a measurement approach, it is investigated to how to contain the environment reflection in a dynamic on-body UWB channel model. Moreover, the influence of a metal floor or indoor environment on the communication performance is also evaluated by computer simulation.

Manuscript received December 29, 2010.
Manuscript revised April 18, 2011.

[†]The authors are with the Graduate School of Engineering, Nagoya Institute of Technology, Nagoya-shi, 466-8555 Japan.
a) E-mail: wang@nitech.ac.jp

DOI: 10.1587/transcom.E94.B.2492

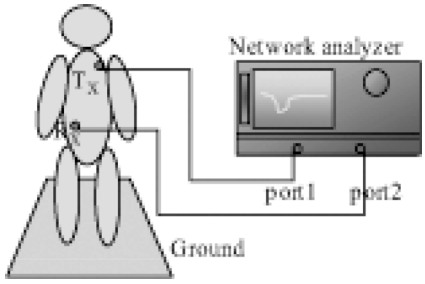

Fig. 1 Measuring system.

2. Measurement Method

Figure 1 shows the measurement system. Two planar UWB antennas (SkyCross Co., SMT-3TO10M-A) were arranged just above the surface of the human body as the transmitter and receiver respectively. The antennas have a planar structure ($13.6 \times 16.0 \times 3.0$ mm) and linear polarization. Their radiation pattern is azimuth omni-directional, and the voltage standing wave ratio (VSWR) is less than 2.0 in free space. However, when they were attached above the surface of human body, the antennas suffered from impedance mismatching with the characteristic impedance. The scattering parameter S21 was therefore measured between the UWB full band from 3.1 GHz to 10.6 GHz with a vector network analyzer. It was found that at most of frequencies the VSWR was still less than 2.0, and the worst VSWR did not exceed 2.8. This VSWR characteristic should be allowable for acting as an on-body antenna. Moreover, the coaxial cables were arranged to be orthogonal to the antenna polarization in order to minimize the influence from the cables. The measurement was conducted in a semi-anechoic chamber with a metal floor as a reflection object. This facilitate the extraction of feature in order to contain the environment reflection.

3. Channel Modeling

As a typical situation of healthcare applications, the distance between the two antennas was fixed at 0.5 m by arranging the transmitting antenna in the left chest and the receiving antenna in the right waist. 81 measured data of S_{21} in total, in nine typical postures such as standing upright and walking for nine persons, were obtained. Because measured S_{21} data correspond to the transfer function in the frequency

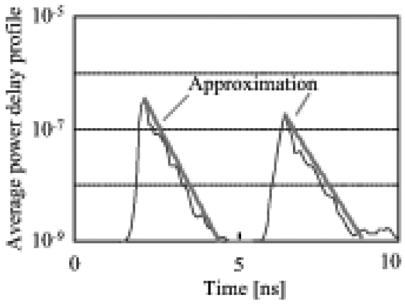

Fig. 2 Average power delay profile.

domain, the impulse response $h(t)$ was calculated by the inverse Fourier transform of them, and the power delay profile $p(t)$ was obtained from the following equation

$$p(t) = \langle h^*(t) \cdot h(t) \rangle \tag{1}$$

where * denotes the complex conjugate and $\langle \cdot \rangle$ denotes the statistical average for the postures. Hamming window was used in the inverse Fourier transform in order to limit the signal to effective frequency components (11 GHz at maximum) and detect small power spectra. The time resolution of the inverse Fourier transform for $h(t)$ can be approximated as the reciprocal (1/11 GHz = 0.09 ns) multiplied by the additional window function bandwidth. Since the coefficient of Hamming window is 2, this results in a 0.18-ns time resolution for the impulse response and the power delay profile.

Figure 2 shows the temporal waveform of the average power delay profile $\bar{p}(t)$ for the nine persons. As can be seen, it consists of two clusters, and more than one multipaths are included in each cluster. The first cluster is related to the diffraction and reflection on the surface of the human body, and the second cluster is due to the reflection from the floor. This conclusion was derived from two facts. First, if we calculated the arrival time by assuming an image antenna of the metal floor, it was identical to the time interval between the first and second cluster. Second, when we removed the metal floor to form a full anechoic chamber, we did not observe the second cluster.

$\bar{p}(t)$ can be approximated in each cluster by the exponential decay expression with time

$$\bar{p}(t) = A \exp\left(-\frac{t - t_0}{\gamma_t}\right). \tag{2}$$

where t_0 is the time that the first path arrives, A is the value of the average power delay profile at $t = t_0$, and γ_t is the decay time constant. It is found that the decay time constant is 0.36 ns for cluster 1 and 0.43 ns for cluster 2.

Next, in the power delay profile $p(t)$, each peak is assumed to be corresponding to one multipath. The cumulative distributions of the multipath power gain in dB unit, which is actually the attenuation between the transmitting antenna and the receiving antenna, for the first peak of both clusters were shown in Fig. 3. The normal distribution fitting curves with the statistical means μ and standard deviations

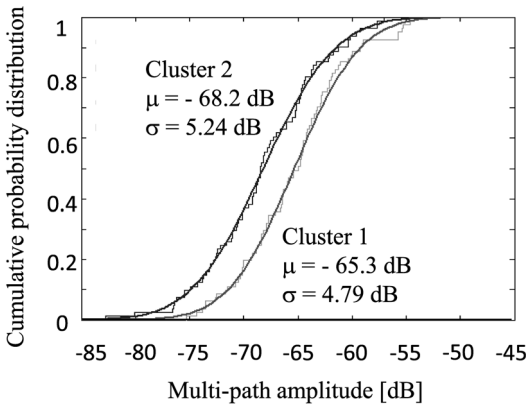

Fig. 3 Statistical distribution of the first peak power.

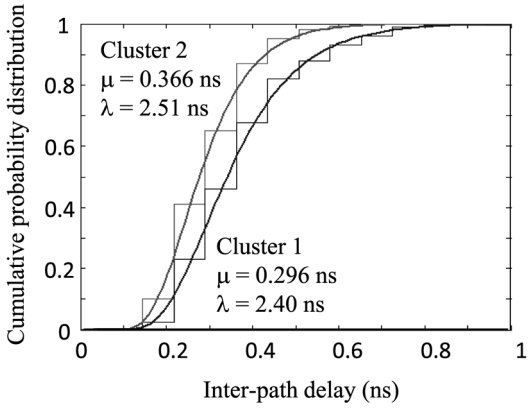

Fig. 4 Statistical distribution of inter-path delay.

σ are also shown in this figure. Good coincidence suggests that the multipath power gain is according to lognormal distribution. Moreover, it is found that the mean attenuation of the first peak is 65 dB when the signal propagates on the human body, and the first peak of the reflected wave from the floor attenuates by 68 dB in a mean value.

On the other hand, the inter-path delay, which corresponds to the temporal delay between two successive multipaths, represents the characteristic of the arrival time for all multipaths in the on-body channel. Figure 4 shows the cumulative distributions for the inter-path delay. Each individual path was determined from the peaks in impulse response $h(t)$ because it had a high temporal resolution of 0.18 ns. Also shown in the figure are the approximation curves of the inverse Gaussian distribution with a mean μ and standard deviation μ^3/λ. Because both are corresponding well, the inter-path delay of multipaths can be concluded to follow the inverse Gaussian distribution. The mean values for cluster 1 and cluster 2 are 0.30 ns and 0.37 ns, respectively.

From the above results, the reflection from the surroundings such as floor is basically able to be separated from the diffraction and reflection on the surface of the human body. It is therefore reasonable to do channel modeling separately for the on-body UWB communications.

4. Model Implementation and Verification

The impulse response is generated based on the previously described characteristics which are extracted from the measured results. That is, it is generated in three steps. (1) The average power of the multipaths in each cluster follows the exponential decay with a time constant γ_t. (2) The variation of multipath power in each cluster follows the lognormal distribution with a standard deviation σ. (3) The variation of inter-path delay follows the inverse Gaussian distribution with a mean μ and a standard deviation μ^3/λ. Figure 5 shows an example of the generated impulse response, in which the main power gain of all multipaths is normalized to one.

The impulse response was generated like this for 50 times, and their statistical characteristic was extracted by using the same way as described above. Table 1 compares the statistical parameters extracted from the measured data and the modeling data. It is found that the modeling results show fair agreement with the measured results. Moreover, Table 2 compares the channel parameters in the presence and absence of the metal floor for cluster 1. The channel parameters in the absence of the floor were measured in a full anechoic chamber as given in [5]. So the only difference between the semi chamber and full chamber in Table 2 is just the metal floor. As can be seen in Table 2, the inter-path delay agrees well. It means that the floor does not produce new multipath components in cluster 1 that are generated by the diffraction and reflection of the human body. Moreover, the multipath power also exhibits the same lognormal distribution, although the standard deviation σ differs 4 dB due to the existence of the metal floor. The difference in σ may be attributed to measurement uncertainty, especially the influence of coaxial cables. Based on these findings, it should be reasonable to regard a complete body area channel model as a combination of the on-body model and the additional components from the environment.

Furthermore, the mean τ_m and the delay spread σ_τ of the power delay profile were calculated for both measured data and modeling data. The cumulative distributions of the delay spread σ_τ in cluster 1 and 2 also agree well between them, which further shows the validation of the proposed channel model.

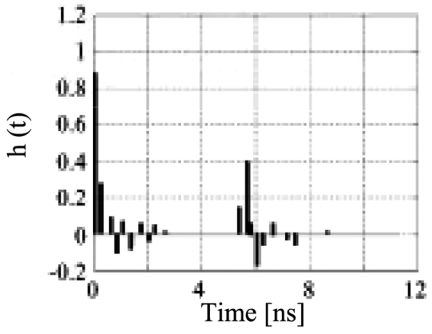

Fig. 5 Example of impulse response.

Table 1 Channel parameters.

	Cluster 1		Cluster 2	
	Meas.	Model	Meas.	Model
(1) σ [dB]	4.79	4.11	5.24	4.68
(2) μ [ns]	0.296	0.325	0.366	0.390
(2) λ [ns]	2.40	1.68	2.51	2.17

(1)Multipath power: Lognormal distribution
(2)Inter-path delay: Inverse Gaussian distribution

Table 2 Comparison of channel parameters for cluster 1.

	Semi chamber	Full chamber
(1) σ [dB]	4.79	8.87
(2) μ [ns]	0.296	0.30
(2) λ [ns]	2.40	2.14

(1)Multipath power: Lognormal distribution
(2)Inter-path delay: Inverse Gaussian distribution

5. BER Performance for UWB-IR

The effect on communication performance of the environment reflection was investigated by computer simulation. The most common and traditional way of emitting an UWB signal is by radiating pulses that are very short in time. This transmission technique goes under the name of impulse radio (IR). For IR-UWB, one of the common ways by which the information data symbols modulate the pulses is the pulse position modulation (PPM). In addition to modulation and in order to shape the spectrum of the generated signal, the data symbols are encoded using pseudo-noise codes. In a common approach, the encoded data symbols introduce a time dither on generated pulses leading to the so-called time-hopping (TH) UWB. In this study, TH-UWB combined with binary PPM (2PPM-TH-UWB) was adopted for the communication performances evaluation.

On the other hand, the optimum receiver for the additive white Gaussian noise (AWGN) channel is not appropriate for the on-body multipath channel since its structure foresees the presence of a correlation that is matched to one single waveform. As it should be, the performance degradation can be mitigated if a detailed characterization of the multipath-affected channel is available. IR-UWB systems can take advantage of multipath propagation by combining different and independent replicas of the same transmitted pulse to improve the BER performance. This is known as the RAKE receiver structure. By comparing the captured energy as a function of the multipath numbers, it is found that 90% of the received energy was captured by the maximum four multipaths in the presence of the floor. A four-finger RAKE receiver was therefore employed in the simulation scheme [8]. Table 3 gives the simulation parameters.

Figure 6 shows the average bit error rate (BER) performance versus Eb/No. For clarifying the influence from the environment, the BER was obtained and compared under channels with both cluster 1 and cluster 2 as well as with only cluster 1. It is found that degradation in the BER performance because of the reflection from the floor is about 2 dB at BER = 0.01. Moreover, achieving a BER of 0.01

Table 3 Simulation parameters.

Transmission speed	50 Mbps
Modulation scheme	2PPM-TH-UWB
Pulse width	100 ps
Chip length	1.25 ns
Chips per bit	16
Receiver structure	RAKE

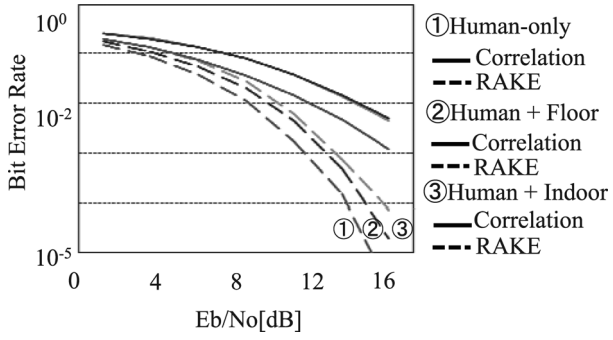

Fig. 6 Average BER performance.

requires a Eb/No of about 14 dB for the conventional correlation receiver, and a Eb/No of about 8 dB for the four-finger RAKE receiver. In addition, a further simulation was done by combining the cluster 1 of the on-body channel and the IEEE802.15.3a CM1 channel [9] for simulating an additional indoor propagation characteristic. The BER degradation compared with the influence from the metal floor is only 1 dB at BER = 0.01. These results suggest that the high-speed transmission of 50 Mbps is possible in the on-body communication situation by the use of the RAKE receiver. Since the transmission speed of 10 Mbps may be enough when limiting it to the application of the healthcare and medical treatment, the influence of the multipath will be weakened and a further improvement of the BER performance can be expected.

6. Conclusions

This study aimed how to contain the environment reflection in a dynamic on-body UWB channel model. In addition to various human body postures, the reflection from the environment such as the floor was included. It has been shown that the environment reflection does not basically affect the multipath components in the first cluster that are generated by the diffraction and reflection of the human body. It is available to establish a body area channel model by a combination of the on-body model and the additional components from the environment. Using the impulse response expression of the channel model generated in such a way, the average BER performance of a typical IR-UWB system has been clarified. It has been found that the degradation at BER = 0.01 is 2–3 dB due to the influence of the reflected waves from the environment. A high-speed transmission of 50 Mbps on the body surface is possible by the use of the RAKE receiver structure.

References

[1] A.W. Astrin, H.-B. Li, and R. Kohno, "Standardization for body area networks," IEICE Trans. Commun., vol.E92-B, no.2, pp.366–372, Feb. 2009.

[2] A. Fort, J. Ryckaert, C. Desset, P. De Doncker, P. Wambacq, and L. Van Biesen, "Ultra-wideband channel model for communication around the human body," IEEE Trans. J. Sel. Areas Commun., vol.24, no.4, pp.927–933, April 2006.

[3] A. Taparugssanagorn, A. Rabbachin, M. Hamalainen, J. Saloranta, and J. Iinatti, "A review of channel modeling for wireless body area network in wireless medical communications," Proc. 11th Int. Symp. on Wireless Personal Multimedia Communications (WPMC'08), Lapland, Finland, FL3-1, Sept. 2008.

[4] H. Sawada, T. Aoyagi, J. Takada, K.Y. Yazdandoost, and R. Kohno, "Channel model for wireless body area network," Presented at Int. Symp. on Medical Information and Commun. Tech. (ISMICT), Yokohama, Japan, Dec. 2007.

[5] Q. Wang, T. Tayamachi, I. Kimura, and J. Wang, "An on-body channel model for UWB body area communications for various postures," IEEE Trans. Antennas Propag., vol.57, no.4, pp.991–998, April 2009.

[6] A.F. Molisch, "Ultrawideband propagation channels — Theory, measurement, and modeling," IEEE Trans. Veh. Technol., vol.54, no.5, pp.1528–1545, Sept. 2005.

[7] A.F. Molisch, D. Cassioli, C.-C. Chong, S. Emami, A. Fort, B. Kannan, J. Karedal, J. Kunisch, H.G. Schantz, K. Siwiak, and M.Z. Win, "A comprehensive standardized model for ultrawideband propagation channels," IEEE Trans. Antennas Propag., vol.54, no.11, pp.3151–3166, Nov. 2006.

[8] Q. Wang and J. Wang, "Performance of ultra wideband on-body communication based on statistical channel model," IEICE Trans. Commun., vol.E93-B, no.4, pp.833–841, April 2010.

[9] J. Foerster, "Path loss proposed text and S-V model information," IEEE P802.15-02/xxxr0-SG3a, pp.833–841, July 2007.